Synthesis and Biological Evaluation of 7-(2-Chlorophenylamino)-5-((2-[^{18}F]fluoro-ethyoxy)methyl)pyrazolo[1,5-*a*]pyrimidine-3-carbonitrile as PET Tumor Imaging Agent

Jingli Xu, Hang Liu, Guixia Li, Yong He, Rui Ding, Xiao Wang, Man Feng, Shuting Zhang, Yurong Chen, Shilei Li, Mingxia Zhao, Yingruo Li, and Chuanmin Qi

Key Laboratory of Radiopharmaceuticals (Beijing Normal University), Ministry of Education, College of Chemistry, Beijing Normal University, Beijing 100875, PR China

Reprint requests to Prof. C. M. Qi. E-mail: qicmin@sohu.com

Z. Naturforsch. **2012**, *67b*, 827 – 834 / DOI: 10.5560/ZNB.2012-0047
Received February 10, 2012

An ^{18}F-labeled pyrazolo[1,5-*a*]pyrimidine derivative, 7-(2-chlorophenylamino)-5-((2-[^{18}F] fluoroethyoxy)methyl)pyrazolo[1,5-*a*]pyrimidine-3-carbonitrile ([^{18}F]**5**), has been designed and prepared as a radio tracer candidate for tumor detection with positron emission tomography (PET). The desired product [^{18}F]**5** was synthesized by nucleophilic substitution of the corresponding tosylated precursor with [^{18}F]KF/Kryptofix 2.2.2 and potassium carbonate in anhydrous DMF at 100 °C for 20 min followed by purification with HPLC. The radiochemical purity was > 98 %, and the radio-chemical yield was 25 % (decay-uncorrected). Compound [^{18}F]**5** was very stable *in vitro*. The biodistribution study in mice bearing S180 tumors demonstrated that [^{18}F]**5** had a rapid and prolonged accumulation in tumors with moderate washout from other tissues.

Key words: Pyrazolo[1,5-*a*]pyrimidine Derivative, 7-(2-Chlorophenylamino)-5-((2-[^{18}F]fluoroethyoxy)methyl)pyrazolo[1,5-*a*]pyrimidine-3-carbonitrile, Radiotracer, Tumor Detection, Positron Emission Tomography

Introduction

With the increasing availability of PET (positron emission tomography) to provide quantitative kinetic information of metabolic pathways and physiological processes *in vivo* [1], PET and in particular an integrated PET/CT technique can detect diseases earlier and more accurately than any other imaging technique. A PET/CT is an effective tool to help to stage local, regional, distant diseases and to provide therapeutic guidance for cancer therapy. 2-[^{18}F]Fluoro-2-deoxyglucose (^{18}F-FDG), an analog of glucose, is the most widely used compound for cancer detection [2, 3]. In spite of being a very effective PET tracer for many types of tumors, with ^{18}F-FDG it is often difficult to differentiate tumor from inflammatory cells, especially for brain tumors because of the high background in the brain, and its low uptake in tumors that are growing slowly can cause false-negative results [4, 5]. Considering the drawbacks of using FDG for tumor imaging and the advantages of fluorine-18 as an ideal positron-emitting radionuclide (relatively longer half-life (110 min), comparable size to H atoms and lower energy), several new agents radiolabeled with ^{18}F that are under investigation or have found clinical use in cancer management [6].

Pyrazolo[1,5-*a*]pyrimidine derivatives display extensive pharmaceutical activity due to the structural similarity of the pyrazolo[1,5-*a*]pyrimidine ring system to purine, and the latter exerts antimetabolic activity in biochemical reactions [7]. Furthermore, the pyrazolo[1,5-*a*]pyrimidine core structure has several positions for introducing a substituent, the C-5 and the C-7 position have commonly been used for introducing substituents in anti-tumor drug design [8 – 13]. Recently, a series of novel 3-cyano-5,7-disubstituted pyrazolo[1,5-*a*]pyrimidine derivatives with various C-7 aniline substituents and C-5 amino alkoxy moieties have been synthesized and showed that pyrazolo[1,5-*a*]pyrimidine analogs of purine have strong anti-cancer activity [9].

We set out to explore a radiolabeled analog of pyrazolo[1,5-*a*]pyrimidine for use as a PET tumor imaging agent. In this study, a novel ^{18}F-labeled

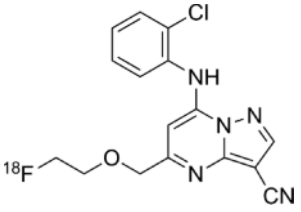

Fig. 1. Structure of the ^{18}F-labeled pyrazolo[1,5-*a*]pyrimidine derivative.

pyrazolo[1,5-*a*]pyrimidine derivative, [^{18}F]**5** (Fig. 1), has successively been synthesized and tested in Kunming Mice bearing S180 tumors. Afterwards, we compared the biodistribution data of [^{18}F]**5** with data obtained using the previously described [^{18}F]FDG and *O*-2-[^{18}F]fluoroethyl-L-tyrosine (L-[^{18}F]FET) [14].

Results and Discussion

Chemistry

Scheme 1 shows the synthetic procedures for **5** and its ^{18}F-labeled analog ([^{18}F]**5**). The synthesis route to **1** followed a procedure described previously [9]. Substitution of 7-Cl in **1** with 2-chloroaniline produced **2**. Treatment of **2** with ethylene glycol in DMF solution using NaH as a base generated **3**. Direct interaction between **3** and toluene sulfonyl chloride provided the precursor **4**. ^{19}F substitution to obtain **5** was achieved from precursor **4** using TBAF·3H$_2$O in dry DMF at 100 °C under nitrogen atmosphere for

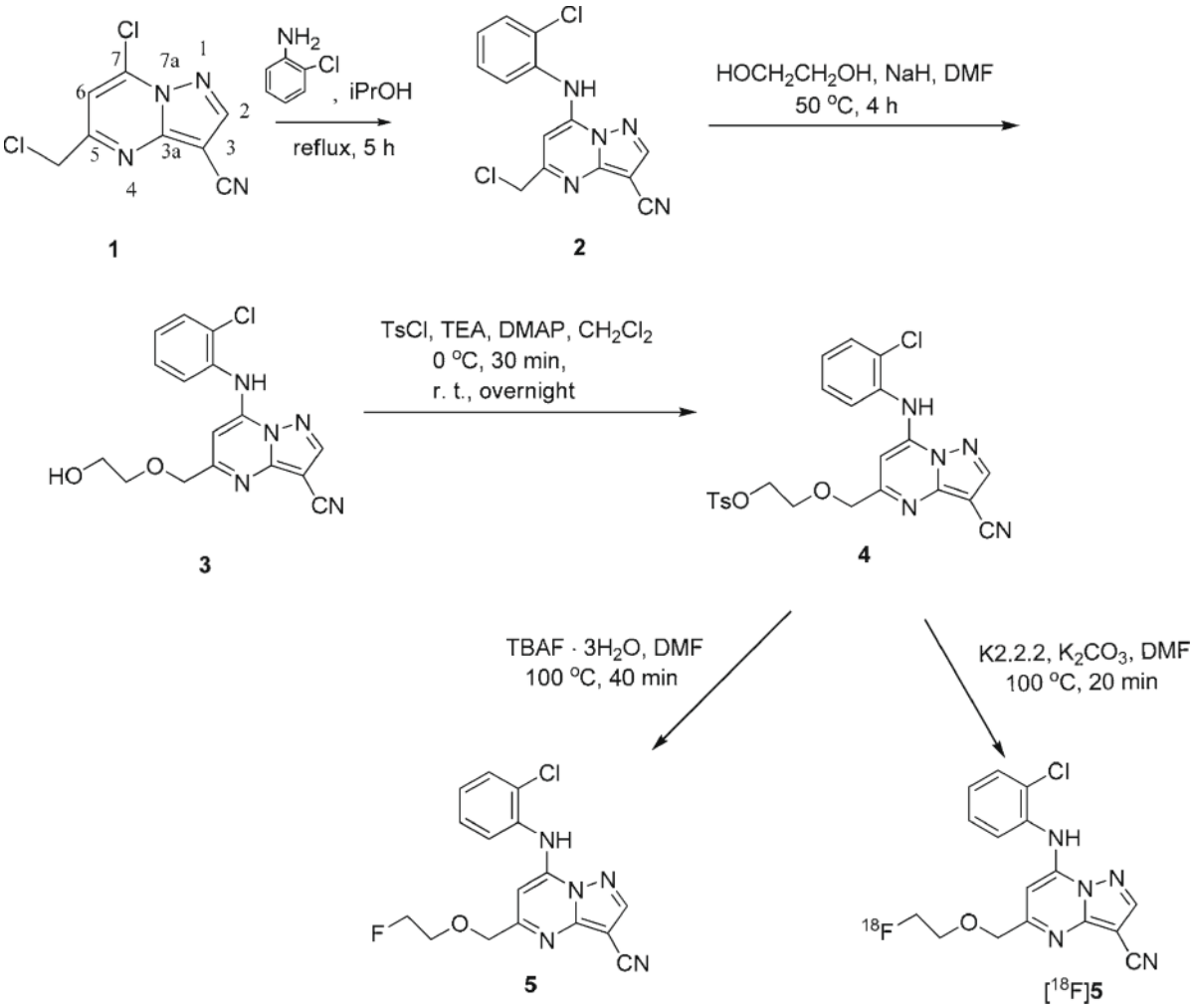

Scheme 1. The synthetic route to **5** and [^{18}F]**5**.

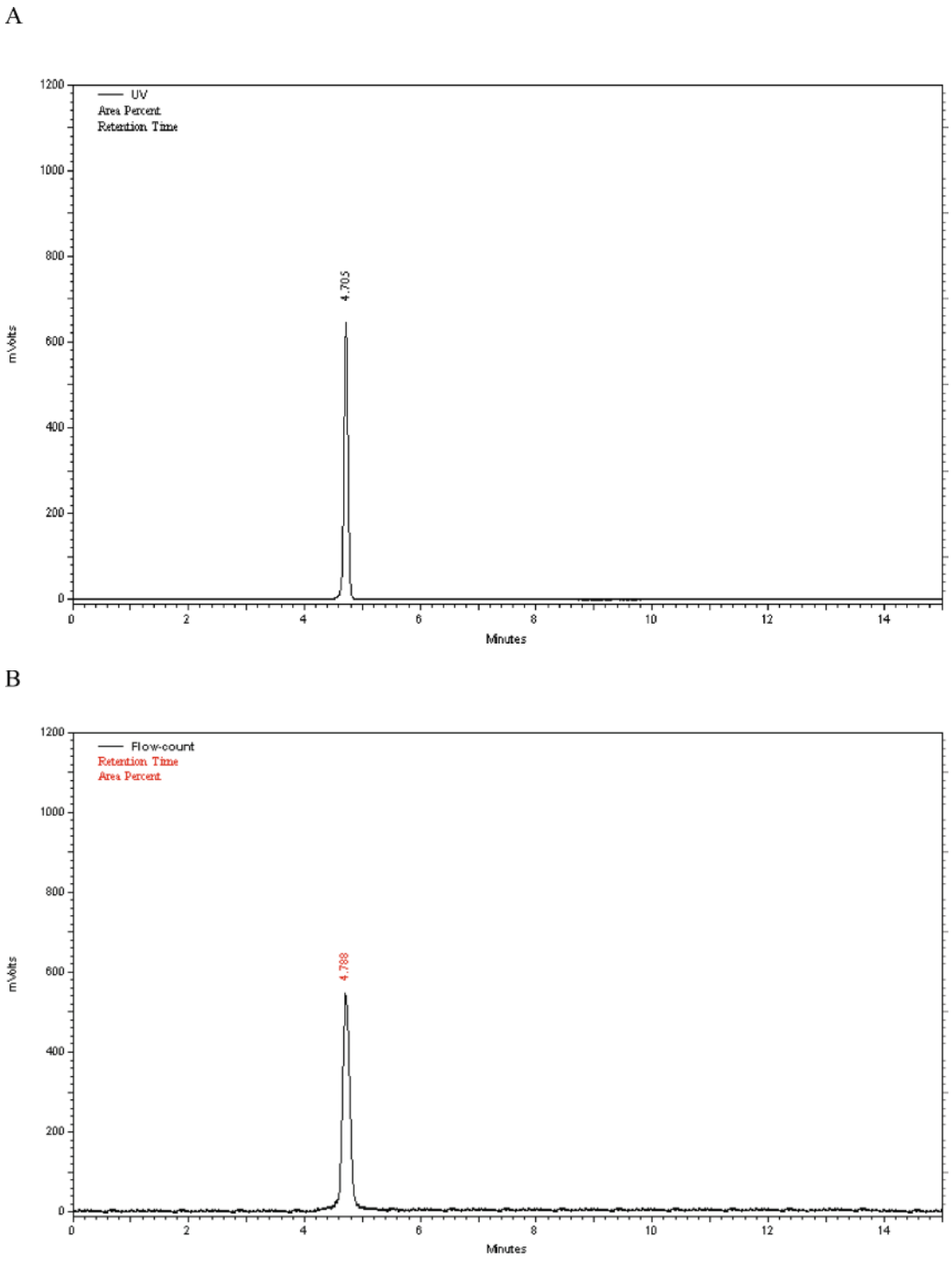

Fig. 2. HPLC profiles of **5** (A) and [^{18}F]**5** (B). HPLC conditions: Alltech system; a Grace Alltima C-18 column (250 × 10 mm i. d.), CH_3CN-H_2O = 70 : 30 (v/v), 3 mL min^{-1}, 245 nm, t_R = 4.70 min (UV), 4.79 min (γ). The slight difference in retention time between the UV peaks is due to the configuration of the detector system.

40 min with 30 % yield. The structure of **5** was characterized by ^{1}H NMR, ^{13}C NMR, ESI-MS, and IR spectroscopy and elemental analysis. The radiosynthesis of [^{18}F]**5** was performed through the corresponding tosylate precursor **4** with no-carrier-added potassium [^{18}F]fluoride and Kryptofix K2.2.2 in anhydrous DMF at 100 °C. [^{18}F]Fluoride incorporation by nucleophilic displacement of the tosylate leaving group in **4** gave [^{18}F]**5** in a moderate overall radiochemical yield of about 25 % (decay-uncorrected) within 60 min including HPLC separation. The desired product [^{18}F]**5** was collected by HPLC, and the solvent was evaporated using a rotary evaporator. The product was dissolved in phosphate-buffered saline solution (pH = 7.4). The radiochemical purity exceeded 98 %. The structure of [^{18}F]**5** was confirmed according to the retention of [^{18}F]**5** (t_R = 4.79 min) which was in good agreement with that of its corresponding F-19 substituted **5** (t_R = 4.70 min), as shown in Fig. 2.

Measurement of the partition coefficient

The partition coefficient (log*P*) value of [^{18}F]**5** was 0.92, suggesting that this radiotracer is lipophilic.

*Stability of [^{18}F]**5** in vitro*

The radio-HPLC showed that the radiotracer is stable in both phosphate-buffered saline (pH = 7.4) and murine plasma at 37 °C after 1 h.

*Biodistribution of [^{18}F]**5** in S180-bearing mice*

The biodistribution data of [^{18}F]**5** is summarized in Table 1. Table 2 shows the comparison of tumor uptake (% ID/g) and the ratios of tumor to brain, muscle and blood among [^{18}F]**5**, [^{18}F]FDGand L-[^{18}F]FET in the same animal model. The biodistribution data of [^{18}F]FDG and L-[^{18}F]FET were taken from our previous report [14].

As shown in Table 1, after a fast distribution, [^{18}F]**5** was excreted from the body mainly through the liver and kidney. The radioactivity of [^{18}F]**5** in the tumor was 2.18 ± 1.02, 3.66 ± 1.41, 2.83 ± 0.18, and 2.12 ± 0.53 % ID/g at 5, 15, 30, and 60 min post-injection (pi), respectively, showing a remarkably increasing uptake of this compound in the tumor. [^{18}F]**5** reached its peak of 3.66 ± 1.41 % ID/g at 15 min pi, and then decreased to 2.12 ± 0.53 % ID/g after 60 min. Nearly 60 % radioactivity was still retained in the tumor after 60 min indicating good persistence in tumor uptake. Meanwhile, the radioactivity of [^{18}F]**5** in other organs and tissues decreased rapidly. The tumor to brain, tumor to muscle and tumor to blood ratios reached high levels of 2.23, 1.14 and 1.30 at 15 min pi, respectively.

As shown in Table 2, [^{18}F]FDG washed out swiftly from the blood resulting in high tumor to blood ratios: 11.38 at 30 min pi and 19.47 at 60 min pi. On the other hand, the high uptake in the brain resulted in low tumor to brain ratios: 0.61 at 30 min pi and 1.02 at 60 min pi. Taking this drawback into account, [^{18}F]FDG is limited in the application as a PET imaging agent of brain tumors [4]. On the contrary, the tumor to blood ratios of L-[^{18}F]FET were much lower, and the tumor to brain ratios were relatively higher: 2.54 at 30 min pi and 2.93 at 60 min pi. Thus, L-[^{18}F]FET is suited as a PET brain tumor imaging agent [14 – 17].

Compared with [^{18}F]FDG and L-[^{18}F]FET, [^{18}F]**5** exhibited a higher absolute radioactivity uptake in tumors than [^{18}F]FDG before 30 min pi and L-[^{18}F]FET before 15 min pi. At 60 min pi all three radiotracers had a similar absolute radioactivity uptake in the tumor.

Organs	Time (min)			
	5	15	30	60
Heart	4.79 ± 1.26	4.24 ± 1.11	3.36 ± 0.47	2.68 ± 0.19
Liver	13.50 ± 4.63	12.20 ± 2.38	9.14 ± 2.01	3.37 ± 0.23
Spleen	4.46 ± 2.14	3.38 ± 1.15	2.63 ± 0.07	1.45 ± 0.29
Lung	3.77 ± 0.75	3.07 ± 0.49	2.99 ± 0.59	1.77 ± 0.39
Kidney	6.61 ± 1.50	4.74 ± 0.93	2.93 ± 0.46	1.90 ± 0.08
Brain	2.22 ± 0.30	1.64 ± 0.50	1.47 ± 0.01	1.20 ± 0.18
Muscle	4.88 ± 1.27	3.22 ± 1.06	2.56 ± 0.55	2.47 ± 0.34
Blood	3.17 ± 1.21	2.81 ± 0.67	2.50 ± 0.25	1.84 ± 0.39
Tumor	2.18 ± 1.02	3.66 ± 1.41	2.83 ± 0.18	2.12 ± 0.53
Tumor/Brain	0.98	2.23	1.93	1.77
Tumor/Muscle	0.45	1.14	1.10	0.86
Tumor/Blood	0.69	1.30	1.13	1.15

Table 1. Biodistribution of [^{18}F]**5** in mice bearing an S 180 tumor, expressed as percent of injected dose per gram (% ID/g ± SD), $n = 4$.

Table 2. Biodistribution comparison of [^{18}F]**5**, [^{18}F]FDG and L-[^{18}F]FET in mice bearing an S 180 tumor, expressed as percent of injected dose per gram (% ID/g ± SD), $n = 4$.

Organs	Compounds	Time (min) 5	15	30	60
Tumor	[^{18}F]**5**	2.18 ± 1.02	3.66 ± 1.41	2.83 ± 0.18	2.12 ± 0.53
	[^{18}F]FDG	1.27 ± 0.54	1.56 ± 0.23	1.86 ± 0.18	2.16 ± 0.34
	L-[^{18}F]FET	2.08 ± 0.49	2.50 ± 0.23	3.28 ± 0.69	2.75 ± 0.36
Tumor/Brain	[^{18}F]**5**	0.98	2.23	1.93	1.77
	[^{18}F]FDG	0.53	0.59	0.61	1.02
	L-[^{18}F]FET	2.10	2.43	2.54	2.93
Tumor/Muscle	[^{18}F]**5**	0.45	1.14	1.10	0.86
	[^{18}F]FDG	0.81	1.37	1.75	2.23
	L-[^{18}F]FET	0.72	0.75	0.62	1.23
Tumor/Blood	[^{18}F]**5**	0.69	1.30	1.13	1.15
	[^{18}F]FDG	1.17	3.42	11.38	19.47
	L-[^{18}F]FET	0.31	0.76	1.02	1.10

The tumor to brain ratios of [^{18}F]**5** were much higher than those of [^{18}F]FDG at all the selected times and were close to those of L-[^{18}F]FET between 15 min and 60 min pi. As shown in Table 2, the tumor uptake and the tumor to brain ratio of [^{18}F]**5** reached their peak at 15 min pi. Meanwhile, the ratio of tumor to muscle also reached its peak (1.14), 1.5 times the uptake of L-[^{18}F]FET (0.75) and close to that of [^{18}F]FDG (1.37); the ratio of tumor to blood also reached its peak (1.3), 1.7 times the uptake of L-[^{18}F]FET (0.76). Taken together, [^{18}F]**5** had the capability to accumulate in the tumor and could enhance the sensitivity in tumor imaging. As a radioactivity tracer, [^{18}F]**5** may be useful for PET imaging of both central and peripheral tumors as well as of metastases of tumors.

Conclusion

The new ^{18}F-labeled pyrazolo[1,5-*a*]pyrimidine derivative [^{18}F]**5** was synthesized by nucleophilic substitution employing tosylate as leaving group and then purified by using reverse phase HPLC. The radiochemical purity of the product was higher than 98 % with radiochemical yields of 25 % (without decay correction). The biodistribution was studied in S180 tumor-bearing mice for comparison of [^{18}F]**5** with [^{18}F]FDG and L-[^{18}F]FET. Compound [^{18}F]**5** showed a higher accumulation in the S180 tumor than [^{18}F]FDG and L-[^{18}F]FET with promising tumor to muscle and tumor to blood ratios, which indicates that further research is needed to develop [^{18}F]**5** and pyrazolo[1,5-*a*]pyrimidine derivatives for potential application in PET tumor imaging.

Experimental Section

All commercial reagents and solvents were used without further purification unless specified. Melting points were determined on an RY-1capillary tube apparatus without correction. ^{1}H NMR spectra were recorded on a Bruker (400 MHz) spectrometer. ^{13}C NMR and ^{19}F NMR spectra were recorded on a Bruker (100 MHz) spectrometer. Tetramethylsilane (TMS) was used as an internal standard. Chemical shift data of the proton resonances (δ) were reported in parts per million relative to the internal standard TMS ($\delta = 0.0$). Mass spectra were obtained using a Bruker Apex IV FTM instrument. Elemental analysis was performed with a Perkin-Elemer 240-C analyzer. IR data were obtained on a Nicolet 360 Avatar infrared spectrophotometer.

The [^{18}F]fluoride used for radiosynthesis was produced by the ^{18}O(p, n)^{18}F nuclear reaction at the Center of Xuanwu Hospital (Beijing, China). Semipreparative HPLC purification was carried out using a semipreparative reversed-phase Grace Alltima^{TM} C18 column (250 × 10 mm, particle size: 10 μm) under the indicated conditions. The semipreparative HPLC system used was an Alltech system with an Alltech HPLC pump Model 626, a Linear UVIS-201, and Bioscan flow-counter. Reversed-phase extraction Sep-Pak C18 Plus cartridges (Waters) were activated with methanol and water before use.

*Synthesis of 5-(chloromethyl)-7-(2-chlorophenylamino)pyrazolo[1,5-a]pyrimidine-3-carbonitrile (**2**)*

7-Chloro-5-(chloromethyl)pyrazolo[1,5-*a*]pyrimidine-3-carbonitrile (**1**), shown in Scheme 1, was synthesized as described previously [9]. A solution of **1** (7.9 g, 35 mmol) in 2-propanol (5 mL) was mixed with 2-chloroaniline (4.7 mL, 45 mmol) and stirred at 60 °C for 3 h. After being cooled to room temperature, the precipitate was filtered, washed thoroughly with isopropanol, and then crystallized from methanol to produce product **2** (9.3 g, 84 % yield) as an orange solid. M. p. 178 – 179 °C. – ^{1}H NMR ($CDCl_3$, 500 MHz): $\delta = 8.38$ (s, 1H, -N*H*Ar), 8.35 (s, 1H, pyrazole-*H*), 7.64 – 7.60 (m, 2H, Ar-*H*), 7.50 – 7.47 (m, 1H, Ar-*H*), 7.39 – 7.36 (m, 1H, Ar-*H*), 6.72 (s, 1H, pyrimidine-*H*), 4.66 (s, 2H, -OCH_2 pyrimidine).

*Synthesis of 7-(2-chlorophenylamino)-5-(2-hydroxyethoxymethyl)pyrazolo[1,5-a]pyrimidine-3-carbonitrile (**3**)*

To a solution of ethane-1,2-diol (0.24 mL, 4 mmol) in anhydrous DMF (5 mL) was added NaH (96 mg, 4 mmol). The suspension was stirred at ambient temperature for 10 min, and then **2** (32 mg, 1 mmol) was added. The mixture was heated at 50 °C for another 4 h, then cooled to room temperature and quenched by addition of H_2O (5 mL). The solid was removed by filtration, and a saturated $NaHCO_3$ solution was added until no more colorless solid was formed. The colorless solid was collected by filtration and subjected to column chromatography on silica gel eluting with 1 : 2 ethyl acetate-petroleum ether (60 – 90 °C) to afford product **3** (18.2 mg, 53 % yield) as a colorless solid. M. p. 157 – 159 °C. – IR (KBr): ν = 3513, 3350, 2891, 2237 (CN), 1629, 1593, 1571, 1435, 1138, 1085 cm^{-1}. – ^{1}H NMR ($CDCl_3$, 500 MHz): $\delta = 8.36$ (s, 1H, pyrazole-*H*), 8.35 (s, 1H, -N*H*Ar), 7.63 – 7.60 (m, 2H, Ar-*H*), 7.48 – 7.44 (m, 1H, Ar-*H*), 7.36 – 7.33 (m, 1H, Ar-*H*), 6.74 (s, 1H, pyrimidine-*H*), 4.72 (s, 2H, –OC*H*$_2$ pyrimidine), 3.84 – 3.81 (m, 2H, HOC*H*$_2$CH$_2$-), 3.74 – 3.72 (m, 2H, HOCH$_2$C*H*$_2$-), 2.18 – 2.15 (m, 1H, *H*OCH$_2$C*H*$_2$-). – ^{13}C NMR ($CDCl_3$, 125 MHz): $\delta = 164.08$ (C-7), 150.30 (C-5), 146.80 (C-2), 145.19 (C-3a), 132.67, 130.87, 128.76, 128.17, 128.09, 124.62 (Ar), 113.23 (CN), 86.99 (C-6), 81. 67 (OCH_2), 73.21 (O*C*H$_2$CH$_2$), 72.65 (C-3), 61.80 (OCH$_2$*C*H$_2$). – MS (EI, 70 eV): m/z (%) = 343 (5) [M]$^+$, 283 (100), 164 (60), 110 (50), 74 (10). – $C_{16}H_{14}ClN_5O_2$ (343.1): calcd. C 55.90, H 4.10, N 20.37; found C 56.03, H 4.19, N 20.22.

*Synthesis of 2-((7-(2-chlorophenylamino)-3-cyanopyrazolo[1,5-a]pyrimidin-5-yl)methoxy)-ethyl-4-methylbenzenesulfonate (**4**)*

To a stirred solution of **3** (0.34 mg, 1 mmol) in CH_2Cl_2 (20 mL) cooled with an ice bath (0 °C) was added Et_3N (0.21 mL, 1.5 mmol), *p*-toluenesulfonyl chloride (TsCl, 0.29 g, 1.5 mmol) and a catalytic amount of 4-dimethylaminopyridine (DMAP, 0.03 g, 0.2 mmol). The reaction was continued at room temperature overnight after 30 min of incubation on ice. The volatile materials were evaporated under vacuum. The crude oily residue was further purified by column chromatography using petroleum ether (60 – 90 °C)-ethyl acetate (5 : 1) as eluant to give product **4** (0.32 g, 64 % yield) as a colorless solid. M. p. 129 – 131 °C. – IR (KBr): $\nu = 3443$, 3310, 2944, 2224 (CN), 1625, 1594, 1573, 1434, 1358, 1191, 1174, 1137, 1026, 925, 775, 751 cm^{-1}. – ^{1}H NMR ($CDCl_3$, 400 MHz): $\delta = 8.32$ (s, 1H, -N*H* Ar), 8.26 (s, 1H, pyrazole-*H*), 7.68 – 7.20 (m, 8H, Ar-*H*), 6.74 (s, 1H, pyrimidine-*H*), 4.52 (s, 2H, -OCH$_2$CH$_2$OC*H*$_2$-), 4.14 – 4.12 (m, 2H, -OC*H*$_2$CH$_2$OCH$_2$-), 3.71 – 3.69 (m, 2H, -OCH$_2$C*H*$_2$OCH$_2$-), 2.35 (s, 3H, -C*H*$_3$). – ^{13}C NMR ($CDCl_3$, 100 MHz): $\delta = 163.59$ (C-7), 150.15 (C-5), 146.68 (C-2), 145.04 (C-3a), 144.96, 132.97, 132.93, 132.68, 130.68, 129.85, 128.54, 128.12, 127.82, 124.17 (Ar), 113.19 (CN), 87.10 (C-6), 81.60 (OCH_2), 73.35 (O*C*H$_2$CH$_2$), 68.80 (C-3), 68.66 (OCH$_2$*C*H$_2$), 21.60 (CH_3). – MS (EI, 70 eV): m/z (%) = 498 (100) [M+H]$^+$, 500 (50), 501 (10), 326 (5). – $C_{23}H_{20}ClN_5O_4S$ (497) calcd. C 55.48, H 4.05, N 14.06; found C 55.53, H 3.90, N 14.22.

*Synthesis of 7-(2-chlorophenylamino)-5-((2-fluoroethyoxy)methyl)pyrazolo[1,5-a]pyrimidine-3-carbonitrile (**5**)*

Tetrabutylammonium fluoride trihydrate (TBAF·3H$_2$O, 0.63 g, 2 mmol) was dissolved in anhydrous CH_3CN (1 mL) and heated rapidly at 120 °C under a nitrogen stream, followed by additional CH_3CN (2 mL). The solvent was evaporated, and this process was repeated three times. After evaporating most of the solvent, a solution of **4** (0.50 g, 1 mmol) in anhydrous DMF (3 mL) was added to the dry reagent. The reaction mixture was stirred at 100 °C for 40 min under a nitrogen stream and cooled to room temperature, then diluted with H_2O (20 mL) and extracted with ethyl acetate (10 mL × 3). The organic layer was dried over Na_2SO_4 and concentrated in a vacuum to obtain a yellow oil. The residue was purified by silica gel chromatography using petroleum ether (60 – 90 °C)-ethyl acetate (6 : 1) as eluant leading to product **5** (0.10 g, 30 % yield) as a colorless solid. M. p. 171 – 172 °C. – IR (KBr): $\nu = 3444$, 3367, 2925, 2231 (CN), 1625, 1599, 1577, 1475, 1311, 1142, 1055 cm^{-1}. – ^{1}H NMR ($CDCl_3$, 400 MHz): $\delta = 8.34$ (s, 1H, pyrazole-*H*), 7.62 – 7.29 (m, 4H, Ar-*H*), 6.84 (s, 1H, pyrimidine-*H*), 4.71 (s, 2H, -OCH$_2$CH$_2$OC*H*$_2$-), 4.66 – 4.54 (dm, 2H, $J = 47.6$ Hz, -CH$_2$C*H*$_2$F), 3.87 – 3.80 (dm, 2H, $J = 30.0$ Hz, -C*H*$_2$CH$_2$F). – ^{13}C NMR ($CDCl_3$, 100 MHz): $\delta = 164.11$ (C-7), 150.32 (C-5), 146.76 (C-2), 145.20 (C-3a), 132.77, 130.77, 128.49, 128.17, 127.88, 124.39 (Ar), 113.22 (CN), 87.02 (C-6), 82.68 (d, $J_{C\text{-}F} = 169.0$ Hz, FCH_2), 81.64 (OCH_2), 73.41 (C-3), 42.57 (d, $J_{C\text{-}F} = 20.0$ Hz, O*C*H$_2$CH$_2$). – ^{19}F NMR ($CDCl_3$, 100 MHz): $\delta = -223.10$. – MS (EI, 70 eV): m/z (%) = 346 (100) [M+H]$^+$, 348 (50), 350 (17). – $C_{16}H_{13}ClFN_5O$ (345) calcd. C 55.58, H 3.79, N 20.26; found C 55.53, H 3.93, N 20.32.

*Synthesis of 7-(2-chlorophenylamino)-5-((2-[^{18}F]fluoroethyoxy)methyl)-pyrazolo[1,5-a]pyrimidine-3-carbonitrile ([^{18}F]**5**)*

[^{18}F]F$^-$ was eluted from the QMA cartridge with 1.3 mL of a Kryptofix 2.2.2 (K222)/K_2CO_3 solution (11 mg of K222 and 3.5 mg of K_2CO_3 in CH_3CN-H_2O 1 mL : 0.3 mL). The solvent was removed at 120 °C under a nitrogen stream. The residue was azeotropically dried with 1 mL of anhydrous CH_3CN at 120 °C under a nitrogen stream. A solution of

the tosylate precursor **4** (5 mg) in anhydrous DMF (1 mL) was added. The mixture was sealed and heated at 100 °C for 20 min and subsequently cooled down. After addition of 10 mL of water the mixture was passed through a Sep-Pak Plus C18 cartridge to remove the Kryptofix 2.2.2 and unreacted potassium [^{18}F]fluoride. The Sep-Pak Plus C18 cartridge was washed with water (10 mL × 2), and the labeled compound was eluted with 2 mL of CH_3CN. The eluted compound was purified by semi-preparative HPLC (Grace C18 column, 250 × 10 mm i. d.); eluant: CH_3CN-H_2O = 70 : 30 (v/v); flow rate: 3 mL min^{-1}; t_R = 4.79 min.

Octanol/water partition coefficient

The partition coefficient was measured as previously described [14]. Each HPLC-purified radiotracer was added to a tube containing 0.5 mL of *n*-octanol and 0.5 mL of phosphate-buffered saline (pH = 7.4). Each phase had been presaturated with the opposite phase. The mixture was vortexed for 1 min and centrifuged at 15 000 rpm for 2 min. Aliquots of both phases were transferred in triplicate to counting tubes and assayed in a γ counter. The partition coefficient was calculated by dividing the radioactivity of the octanol layer by that of the water layer. This measurement was repeated three times.

Stability study

Each HPLC-purified radiotracer (3.7 MBq) was mixed with phosphate-buffered saline (pH = 7.4) at 37 °C for a period of up to 1 h and was analyzed by radio-HPLC. The stability of each HPLC-purified radiotracer in mouse plasma was determined by incubating 0.1 mL of the radiotracer (3.7 MBq) in the solution of 0.5 mL murine plasma at 37 °C for 1 h and 2 h. Plasma proteins were precipitated by adding acetonitrile and removed by centrifugation. The supernatant part was injected into radio-HPLC to determine the stability of the compound.

Biodistribution studies in S180 tumor-bearing mice

All the animal studies were carried out in compliance with relevant national laws relating to the conduct of animal experimentation. Uptake of [^{18}F]**5** in Kunming Mice bearing S180 tumor models were performed according to published methods [14].Briefly, S180 tumor cells were trypsinized, counted, and suspended in a solution containing DMEM and 10% fetal bovine serum. The Kunming Mice were inoculated subcutaneously into the left forelimb with 5×10^6 tumor cells. Studies of tumor uptake were conducted when the tumors reached a size of 0.5 – 0.8 cm in diameter. The tumor-bearing mice were subjected to *in vivo* biodistribution and imaging studies.

Tissue biodistribution studies were conducted by administering, *via* the tail vein, a bolus injection of 370 kBq per mouse in a constant volume of 0.1 mL phosphate-buffered saline solution (pH = 7.4). The animals were sacrificed at 5, 15, 30 and 60 min post injection. The tissues and organs of interest were immediately collected, weighed and measured for ^{18}F radioactivity in a γ counter. Values are expressed as mean ± SD (n = 4).

Acknowledgement

This project was sponsored by the National Natural Science foundation of China (no. 21071022) and the Fundamental Research Funds for the Central Universities. We also wish to thank the cyclotron operator team of the PET Centre of Xuanwu Hospital for providing the fluoride-18 nuclide and technical assistance.

[1] L. Koehler, F. Graf, R. Bergmann, J. Steinbach, J. Pietzsch, F. Wuest, *Eur. J. Med. Chem.* **2010**, *45*, 727 – 737.
[2] L. Fass, *Mol. Oncol.* **2008**, *2*, 115 – 152.
[3] C. K. Hoh, *Nucl. Med. Biol.* **2007**, *34*, 737 – 742.
[4] C. S. Cutler, J. S. Lewis, C. J. Anderson, *Adv. Drug Rev.* **1999**, *37*, 189 – 211.
[5] W. Yu, J. McConathy, L. Williams, V. M. Camp, E. J. Malveaux, Z. Zhang, J. J. Olson, M. M. Goodman, *J. Med. Chem.* **2010**, *53*, 876 – 886.
[6] K. A. Wood, P. J. Hoskin, M. I. Saunders, *Clin. Oncol.* **2007**, *19*, 237 – 255.
[7] L. Varagnolo, M. P. M. Stokkel, U. Mazzi, E. K. J. Pauwels, *Nul. Med. Biol.* **2000**, *27*, 103 – 112.
[8] C. P. Frizzo, E. Scapin, P. T. Campos, D. N. Moreira, M. A. P. Martins, *J. Mol. Struct.* **2009**, *933*, 142 – 147.
[9] J. Li, Y. Zhao, X. Zhao, X. Yuan, P. Gong, *Arch. Pharm. Chem. Life Sci.* **2006**, *339*, 593 – 597.
[10] M. J. Di Grandi, D. M. Berger, D. W. Hopper, C. Zhang, M. Dutia, A. L. Dunnick, N. Torres, J. I. Levin, G. Diamantidis, C. W. Zapf, J. D. Bloom, Y. B. Hu, D. Powell, D. Wojciechowicz, K. Collins, E. Frommer, *Bioorg. Med. Chem. Lett.* **2009**, *19*, 6957 – 6961.
[11] D. Powell, A. Gopalsamy, Y. D. Wang, N. Zhang, M. Miranda, J. P. McGinnis, S. K. Rabindran, *Bioorg. Med. Chem. Lett.* **2007**, *17*, 1641 – 1645.
[12] A. Gopalsamy, H. Yang, J. W. Ellingboe, H.-R. Tsou, N. Zhang, E. Honores, D. Powell, M. Miranda, J. P. McGinnis, S. K. Rabindran, *Bioorg. Med. Chem. Lett.* **2005**, *15*, 1591 – 1594.

[13] A. Gopalsamy, G. Ciszewski, Y. Hu, F. Lee, L. Feldberg, E. Frommer, S. Kim, K. Collins, D. Wojciechowicz, R. Mallon, *Bioorg. Med. Chem. Lett.* **2009**, *19*, 2735 – 2738.

[14] J. L. Xu, H. Liu, G. X. Li, Y. He, R. Ding, X. Wang, M. Feng, S. T. Zhang, Y. R. Chen, S. L. Li, M. X. Zhao, C. M. Qi, Y. H. Dang, *Bioorg. Med. Chem. Lett.* **2011**, *21*, 4736 – 4741.

[15] H. J. Wester, M. Herz, W. Weber, P. Heiss, R. Senekowitsch-Schmidtke, M. Schwaiger, *J. Nucl. Med.* **1999**, *40*, 205 – 212.

[16] P. Heiss, S. Mayer, M. Herz, H. J. Wester, M. Schwaiger, R. Senekowitsch-Schmidtke, *J. Nucl. Med.* **1999**, *40*, 1367 – 1373.

[17] W. A. Weber, H.-J. Wester, A. L. Grosu, M. Herz, B. Dzewas, H.-J. Feldmann, M. Molls, G. Stöcklin, M. Schwaiger, *Eur. J. Nucl. Med. Mol. Imaging* **2000**, *27*, 542 – 549.